Journal of Mathematics Research; Vol. 5, No. 3; 2013
ISSN 1916-9795 E-ISSN 1916-9809
Published by Canadian Center of Science and Education

On the Influence of Radiation and Heat Transfer on an Unsteady MHD Non-Newtonian Fluid Flow with Slip in a Porous Medium

J. A. Gbadeyan[1] & M. S. Dada[1]

[1] Department of Mathematics, University of Ilorin, Ilorin, Nigeria

Correspondence: M. S. Dada, Department of Mathematics, University of Ilorin, Ilorin, Nigeria. E-mail: dadamsa@gmail.com

Received: March 13, 2013 Accepted: July 3, 2013 Online Published: July 23, 2013

doi:10.5539/jmr.v5n3p40 URL: http://dx.doi.org/10.5539/jmr.v5n3p40

Abstract

Radiation and heat transfer effects on a MHD non-Newtonian unsteady flow in a porous medium with slip condition are investigated. The fluid is assumed not to absorb its own emitted radiation but that of the boundaries. The resulted governing equations are non-dimensionalised, simplified and solved using Crank Nicolson type of finite difference method. The numerical results for the velocity and temperature are illustrated graphically and discussed while the skin friction and Nusselt number were also calculated.

Keywords: non-Newtonian, heat transfer, slip condition

1. Introduction

Although, the non-Newtonian behaviour of many fluids has been recognised for a long time, the science of rheology is still in its infancy in many respects. As such, new phenomena are being discovered on a constant basis with new theories propounded. Advancement in computational techniques are making possible much more detailed analyses of complex flow and complicated simulations of the structural and molecular behaviour that give rise to non-Newtonian behaviours. Engineers, Chemists, Physicists and Mathematicians are actively pursuing research in rheology. The large volume of research work on Newtonian fluid is due to the simplified (linear) relation between the shear stress and the velocity gradient in the flow field. However the analysis of non-Newtonian fluid flow field is more complicated because the relationship between the stress and the velocity gradient is non-linear. This fact accounts for the scarce publication on non-Newtonian fluid flow. However a number of industrial fluids exhibit non-Newtonian behaviour such as coal water or coal oil, paints, various polymer solution, slurries, ink soap, food products, suspension of various solid and so on. Moreover, the vast number of fluid flow in a porous media exhibits the non-Newtonian fluid flow behaviour. These important reasons and many other have led some researchers to carry out investigations on the non-Newtonian fluid. For example, Okoya (2008) investigated the transition for a generalised couette flow of a reactive third-grade fluid with viscous dissipation. The disappearance of criticality for a reactive third-grade fluid with Reynold's model viscosity in a flat channel was also studied later by Okoya (2011). An analytic solution of MHD flow and heat transfer for two types of viscoelastic fluid over a stretching sheet with energy dissipation, internal heat source and thermal radiation was obtained by Chen (2010).

H. T. Chen and C. K. Chen (1988) carried out an investigation on free convection of non-Newtonian fluids along a vertical plate embedded in a porous medium. Mehta and Rao (1994) have considered the buoyancy-induced flow of non-Newtonian fluids in porous medium past a vertical plate with non-uniform surface heat flux. A more comprehensive review of the work on non-Newtonian fluid flow in a porous medium can be found in Chamkha (2007).

In addition, the study of thermal convection in porous media has been the subject of many investigations during the past several decades. This is due to the facts that a wide range of geophysical and engineering application of interest consist of porous media. Ranganathan and Viskanta (1984) have studied mixed connection boundary layer flow along a vertical surface in porous medium. Hsieh and Chen (1993) and Armaly presented non-similarity solution for mixed surfaces in a porous medium while Chamkha (2007) studied heat and mass transfer for a non Newtonian fluid flow along a surface embedded in a porous medium with uniform wall heat and mass fluxes and heat generation or absorption. The fluid is assumed to be non-Newtonian power-law and implicit iterative finite difference method was employed to solve the problem.

The study of an electrically conducting fluid flow of non-Newtonian fluid has also gained increasing research interest due to its applications in many biological and engineering problems such as in plasma studies, nuclear reactors, geothermal energy extraction and blood flow problems to mention but a few. Eldabe, Hassan, and Mohammed (2003) carred out an analysis of the effects of couple stresses on the MHD of a non-Newtonian unsteady flow between two parallel porous plates using the Eyring Powell model of the first and second order approximations. The effects of radiation and heat transfer were neglected. However, radiation and heat transfer effects are significant in some industrial applications such as glass production, furnace design in space technology application etc.

The modelling of radiative fluid flow is also significant from the points of view of geophysics, engineering and astrophysics. It has several physical applications such as in some matters at high temperature. Chamkha, Tarkar, and Soundalgekar (2001) analyzed the effects of radiation on free convection flow past a semi-infinite vertical plate with mass transfer. Mehta and Rao (1994) considered the effects of radiation on free convection past a horizontal plate with variable wall temperature and embedded in a non-Newtonian fluid saturated porous medium. Mohanmmadein and El-Amin (2000) studied mixed convection flow over a horizontal plate in a porous medium. Each of the above studies centres on either non-Newtonian fluid without considering the influence of heat transfer or on Newtonian fluid with radiation and heat transfer considered. Resently, Adesanya, and Gbadeyan (2011) studied heat transfer in steady, MHD visco-elastic oscillatory flow with slip through a porous medium using Eyring Powell model with first approximation thereby linearizing the governing equation. Most recently, the problem of free convection in a non-Newtonian fluid along a horizontal plate embedded in a porous medium with internal heat generation was studied by Shobba and Chendrashakkar (2012).

In this present paper, we are interested in the radiation and heat transfer of an unsteady MHD non-Newtonian fluid flow in a porous medium with slip condition using the Eyring Powell model of higher order approximation thereby solving the unsteady non-linear problem. The analysis of the porous medium is based on a Darcian type of model and the fluid slip condition is at the lower wall. The radiation in the fluid is restricted to optically thin limit case.

The rest of the paper is organised as follow: Section 2 deals with the formulation of the problem. In section 3 the numerical method and their discussions are presented. Section 4 contains results and discussion. Finally, in Section 5 some concluding remarks are presented.

2. Mathematical Formulation

Consider a non-Newtonian viscous incompressible and electrically conducting fluid bounded by two stationary parallel plates separated by a distance h apart. The flow is assumed to be unsteady and the channel is filled with saturated porous medium. The Eyring-powell model for describing the shear of a non-Newtonian flow can be used in some cases to describe the viscous behaviours of polymer solutions and the viscoelastic suspensions over a wide range of shear rates (couple stress). The x'-axis is taken along the plate in the vertical upward direction and the y' -axis is normal to the plate in the direction of the applied uniform magnetic field. Then, the fully developed flow is governed by the following set of equations:

$$\frac{\partial u'}{\partial t'} = -\frac{1}{\rho}\left(\frac{\partial P'}{\partial x'} - \frac{\partial \tau_{ij}}{\partial y'}\right) - \frac{\nu u'}{\kappa} + g\beta(T' - T_0') - \frac{\sigma B_0^2 u'}{\rho} \tag{1}$$

$$\rho c_p \frac{\partial T'}{\partial t'} = \kappa \frac{\partial^2 T'}{\partial y'^2} - \frac{\partial q_r}{\partial y'} \tag{2}$$

with associated boundary conditions

$$\begin{array}{llll} u' = 0, & T' = T_0', & y \in (0,h), & t' = 0 \\ u' = \lambda \frac{\partial u'}{\partial y'}, & T' = T_0', & y' = 0, & t' > 0 \\ u' = 0, & T' = T_w', & y' = h, & t' > 0 \end{array}$$

where u' is a velocity component in x-direction, ρ is the density, g is the acceleration due to gravity, T' is the temperature of the fluid, c_p is the specific heat at constant pressure, P' is the pressure inside the fluid, β is the coefficient of thermal expansion, κ is the thermal conductivity, q_r is the radiative flux and σ is the electrical conductivity. ν is kinematic viscosity, μ is the viscosity of the fluid, h is the heat transfer coefficient, B_0 is the strength of the magnetic field and the stress tensor in the Eyring-powell model for non-Newtonian fluid is of the form

$$\tau_{ij} = \mu \frac{\partial u'}{\partial y'} + \frac{1}{\alpha} sinh^{-1}\left(\frac{1}{c}\frac{\partial u'}{\partial y'}\right)$$

μ is the viscosity coefficient, α and c are the characteristics of the Eyring-powell model. The velocity and temperature distributions of the fluid are to be determined for some values of the fluid parameters. The Eyring-powell model in its second order approximation takes the form

$$\tau_{ij} = \mu \frac{\partial u'}{\partial y'} + \frac{1}{\alpha c}\left(\frac{\partial u'}{\partial y'} - \frac{1}{6c^2}\left(\frac{\partial u'}{\partial y'}\right)^3\right), \tag{3}$$

In the optically thin limit case, the fluid does not absorb its own emitted radiation which implies that there is no self-absorption but rather the fluid absorbs radiation emitted by the boundaries. For non-grey gas near equilibrium in the optically thin limit case, Cogley, Vincenti, and Gillies (1968) showed that

$$\frac{\partial q_r}{\partial \hat{y}} = 4L(T' - T'_0) \tag{4}$$

where $L = \int_0^\infty k_{\lambda w}(\frac{de_{b\lambda}}{d\hat{T}})_w d\lambda$, $k_{\lambda w}$ is the absorption coefficient, $e_{b\lambda}$ is the planck function and the subscript w indicates the values at the wall.

The following non-dimensional quantities are adopted:

$$x = \frac{x'}{h},\ y = \frac{y'}{h}, t = \frac{t'u'_0}{h}, \theta = \frac{T' - T'_0}{T'_w - T'_0}, P = \frac{P'}{\rho u'^2_0},\ u = \frac{u'}{u'_0} \tag{5}$$

Using Equations (3), (4) and the set of the non-dimensional quantities (5), Equations (1) and (2) respectively yields

$$Re\frac{\partial u}{\partial t} = -Re\frac{\partial P}{\partial x} + \left(1 + M - N\left(\frac{\partial u}{\partial y}\right)^2\right)\frac{\partial^2 u}{\partial y^2} + Gr\theta - \left(H^2 + K_m\right)u \tag{6}$$

$$RePr\frac{\partial \theta}{\partial t} = \frac{1}{Pr}\frac{\partial^2 \theta}{\partial y^2} - C\theta \tag{7}$$

where $M = \frac{1}{\alpha\mu c}$, $N = \frac{u'^2_0}{2c^3\alpha\mu h^2}$, $K_m = \frac{h^2}{\kappa}$, $\nu = \frac{\mu}{\rho}$, $Pr = \frac{c_p\nu\rho}{\kappa}$ is the Prandtl number, $C = \frac{4Lh^2}{\kappa}$ is the radiation parameter, $Re = \frac{hu'_0}{\nu}$ is the Reynold number, $H = B_0 h\sqrt{\frac{\sigma}{\rho\nu}}$ is the Hartman number and $Gr = \frac{h^2 g\beta}{U'_0\nu}(T'_w - T'_0)$ is the Grashof number as in Devika, Narayana, and Venkataramana (2013). Equations (6) and (7) subjected to the following corresponding dimensionless boundary conditions.

$$\begin{array}{llll} u = 0, & \theta = 0, & y \in (0,1), & t = 0 \\ u = s\frac{\partial u}{\partial y}, & \theta = 0, & y = 0, & t > 0 \\ u = 0, & \theta = 1, & y = 1, & t > 0 \end{array}$$

where $s = \frac{\lambda}{h}$.

The skin friction and Nusselt number are respectively expressed in dimensionless forms as

$$\tau = -\frac{\partial u}{\partial y}\Big|_{y=0} \tag{8}$$

$$Nu = -\frac{\partial \theta}{\partial y}\Big|_{y=0} \tag{9}$$

3. Numerical Method

In other to solve the unsteady non-linear coupled partial differential Equations (6) and (7) with the associated boundary conditions, an implicit finite difference technique of Crank-Nicolson type which is known to converge rapidly and unconditionally stable is employed. The discretized finite difference equations corresponding to Equations (6) and (7) using the method are as follows:

$$\frac{u_i^{n+1} - u_i^n}{\Delta t} = -k_p + \frac{D_i}{Re}\frac{u_{i-1}^{n+1} - 2u_i^{n+1} + u_{i+1}^{n+1} + u_{i-1}^n - 2u_i^n + u_{i+1}^n}{2(\Delta y)^2} + \frac{Gr}{Re}\left(\frac{\theta_i^{n+1} + \theta_i^n}{2}\right) - \frac{H^2 + K_m}{Re}\left(\frac{u_i^{n+1} + u_i^n}{2}\right) \tag{10}$$

$$RePr\frac{\theta_i^{n+1}-\theta_i^n}{\Delta t} = \frac{\theta_{i-1}^{n+1}-2\theta_i^{n+1}+\theta_{i+1}^{n+1}+\theta_{i-1}^n-2\theta_i^n+\theta_{i+1}^n}{2(\Delta y)^2} - C\left(\frac{\theta_i^{n+1}+\theta_i^n}{2}\right) \tag{11}$$

where the pressure gradient (k_p) is assumed to be constant and $D_i = \left(1+M-N(\frac{u_{i+1}^n-u_{i-1}^n}{2\Delta y})^2\right)$.

The associated boundary conditions may be expressed as

$$\begin{array}{lll}
u_i^{n+1}=0, \theta_i^{n+1}=0, & u_i^n=0, \theta_i^n=0, & for\ all\ i, t=0\\
u_{i-1}^{n+1}=-2s\Delta y u_i^{n+1}+u_{i+1}^{n+1}, & \theta_{i-1}^{n+1}=0, & i=1, t>0\\
u_{i-1}^{n}=-2s\Delta y u_i^{n}+u_{i+1}^{n}, & \theta_{i-i}^{n}=0, & i=1, t>0\\
u_i^{n+1}=0, \theta_i^{n+1}=1, & u_i^n=0, \theta_i^n=1, & i=m, t>0
\end{array}$$

where u_0 and θ_0 are the velocity and temperature respectively at $y=0$, u_m and θ_m are the velocity and temperature respectively at $y=1$ and the interval $\Delta y=\frac{1}{m}$.

Equations (10) and (11) may be written respectively as follows:

$$\begin{aligned}
& -r_i u_{i-1}^{n+1} + \left(1+2r_i+(H^2+K_m)v)\right) u_i^{n+1} - r_i u_{i+1}^{n+1}\\
= \ & vGr(\theta_i^{n+1}+\theta_i^n) + r_i u_{i-1}^n + \left(1-2r_i-(H^2+K_m)v)\right) u_i^n + r_i u_{i+1}^n - \Delta t k_p
\end{aligned} \tag{12}$$

$$-R_2\theta_{i-1}^{n+1} + (1+2R_2+C_1)\,\theta_i^{n+1} - R_2\theta_{i+1}^{n+1} = R_2\theta_{i-1}^n + (1-2R-C_1)\,\theta_i^n - R_2\theta_{i+1}^n \tag{13}$$

where $r_i=\frac{\Delta t D_i}{2(\Delta y)^2 Re}$, $v=\frac{\Delta t}{2Re}$, $C_1=\frac{C\Delta t}{2PrRe}$, $R_2=\frac{\Delta t}{2(\Delta y)^2 PrRe}$.

The subscript i and superscript n denote the grid points along the y- and t-directions respectively. The values of u and θ are known at all grid points at $t=0$ from the initial conditions. The computation of u and θ at the (n+1)th time using the values at previous (n)th time are carried out as follows:

At all grid points, the values of θ and u at time $t=0$ from the initial conditions are known. The values of θ at next time step's lenght are calculated using the already known values at previous time as follows: The finite difference Equation (13) forms a tri-diagonal system of equations where the values of θ at every nodal point at next time step length are determined using the known values at previous time. Thomas algorithm is used to solve this tri-diagonal system of equations. As such, the values of θ at every nodal point at this particular time are known. The known values of θ at this particular time are used in Equation (12). Similarly, the values of u are computed at that particular time. The values of u and θ are obtained for the required time following this procedure.

4. Results and Discussion

In order to report on the analysis of the fluid flow, the numerical computations are carried out for various values of Prandtl number (Pr), Hartman number (H), Radiation parameter (C), Grashof number (Gr), the non-Newtonian parameters (M) and (N). Figures 1 and 2 show the velocity distribution profiles with variation of non-Newtonian parameters N and M respectively with other parameters being kept constant. It is observed that as parameter N decreases, the velocity profile decreases slightly. However, the velocity profile decreases appreciably as the value of parameter M increases. It is clear that the parameter M accounts for the low rate of flow of Non-Newtonian fluid when compared with Newtonian fluid flow since the parameter M significantly reduces the velocity of the flow. It also shows that the presence of permeability parameter K_m increases the resistance of the porous medium, thus decreasing the velocity of the flow.

Figures 3, 4 and 5 depict the velocity distribution profiles with variation of Hartman (H), Grashof (Gr) numbers and the porosity parameter K_m respectively. An increase in either K_m or the Hartman number causes a drop in the velocity of the fluid as shown in Figures 3 and 5. It can be seen in Figure 4 that reducing the value of Grashof (Gr) number causes a fall in the velocity the fluid. The effect of transverse magnetic field on an electrically conducting fluid slows down the motion of the fluid. It agrees with the fact that the effect of increasing the Grashof number is to increase the values of velocity profiles.

Figures 6 and 7 show the velocity distribution and thermal profiles with variation of time respectively keeping all other parameters constant. It can be seen that the velocity and temperature of the fluid increases as the time increases towards a steady state.

Figures 8 and 9 illustrate the thermal distribution profiles with the variation of Prandtl number (Pr) and radiation parameter (C) respectively. It is observed that reducing either the Prandtl number or radiation parameter produces significant increase in the thermal condition of the fluid. Thermal conductivity is accelerated with small values of prandtl number thus causing rapid diffusion of heat for smaller Prandtl number than for higher values of Prandtl number.

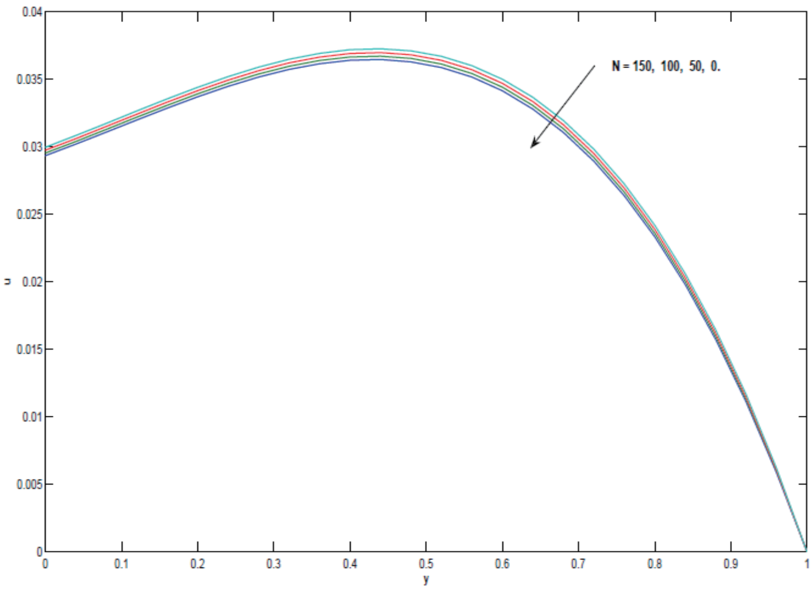

Figure 1. The velocity distribution profiles with variation of parameter N at time $t = 1$ and for fixed parameters $Pr = 1.0,\ C = 1,\ Gr = 10,\ H = 1,\ Re = 1,\ K_m = 0.1$ and $M = 20$

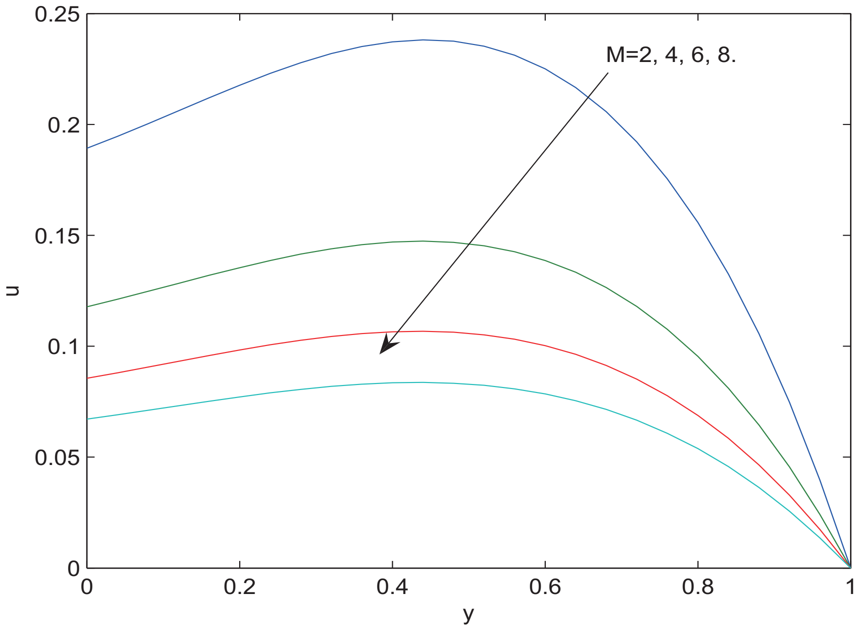

Figure 2. The velocity distribution profiles with variation of parameter M at time $t = 1$ and for fixed parameters $Pr = 1.0,\ C = 1,\ Gr = 10,\ H = 1,\ Re = 1,\ K_m = 0.1$ and $N = 0.05$

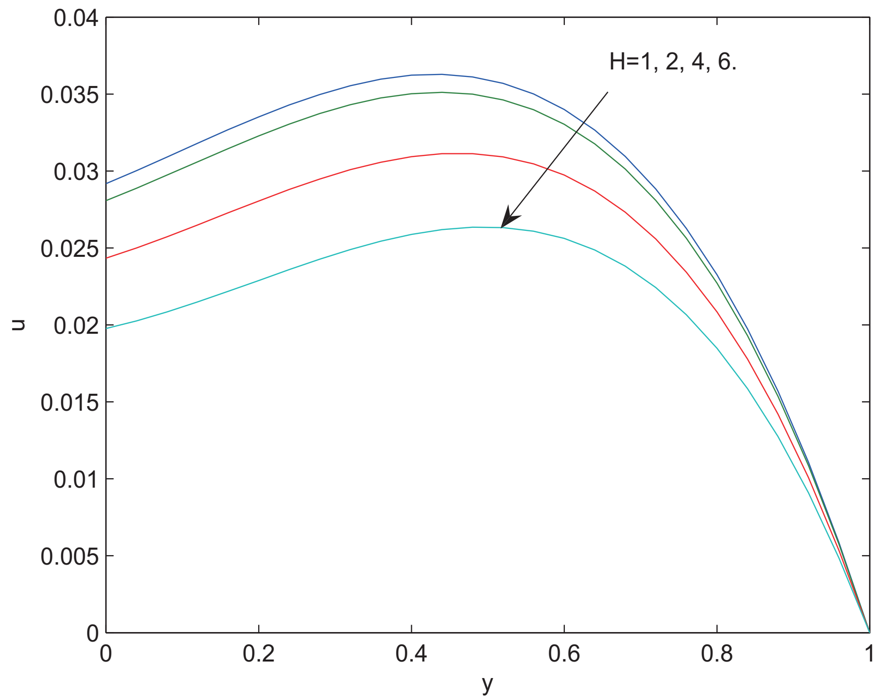

Figure 3. The velocity distribution profiles with variation of Hartman number H at time $t = 1$ and for fixed parameters $Pr = 1.0,\ C = 1,\ Gr = 10,\ M = 20,\ Re = 1,\ K_m = 0.5$ and $N = 0.05$

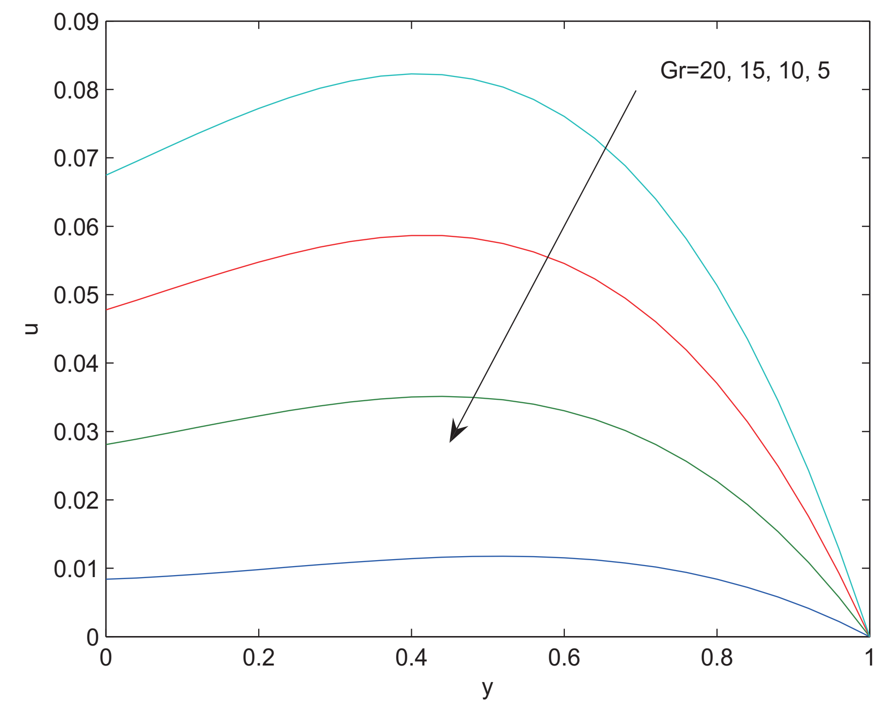

Figure 4. The velocity distribution profiles with variation of Grashof number Gr at time $t = 1$ and for fixed parameters $Pr = 1.0,\ C = 1,\ M = 20,\ H = 1,\ Re = 1,\ K_m = 0.1$ and $N = 0.05$

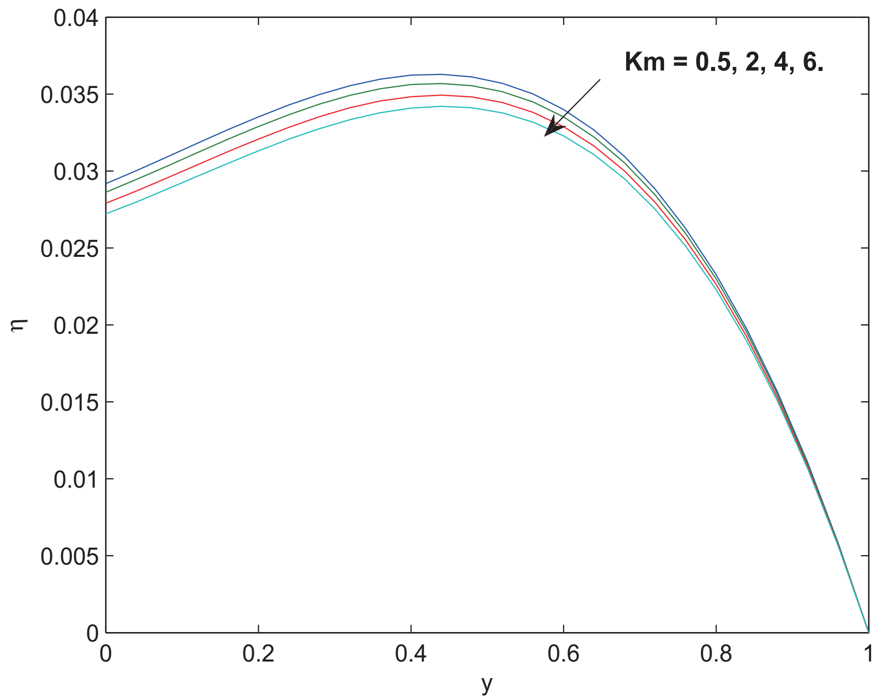

Figure 5. The velocity distribution profiles with variation of parameter K_m at time $t = 1.0$ and for fixed parameters $Pr = 1.0,\ C = 1,\ M = 20,\ H = 1,\ Re = 1,\ Gr = 10$ and $N = 0.05$

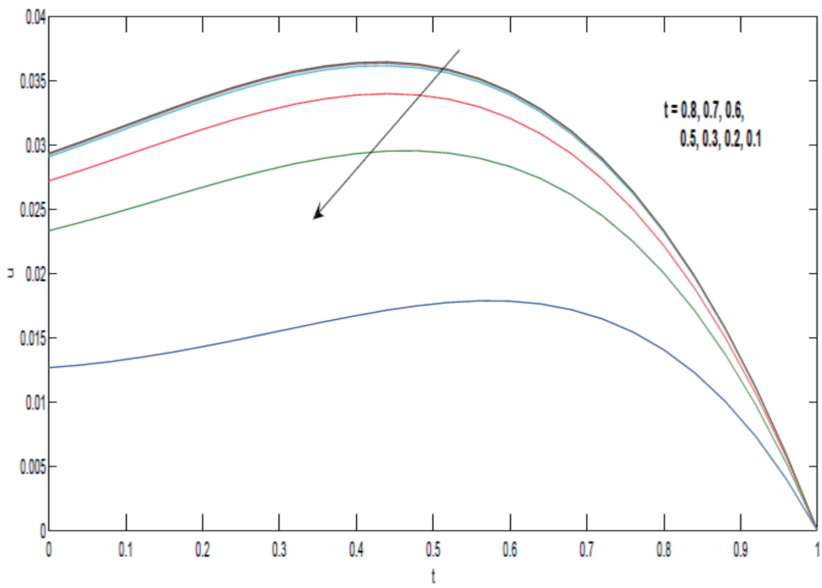

Figure 6. The velocity distribution profiles with variation of time for fixed parameters $Pr = 1.0,\ C = 1,\ M = 20,\ H = 1,\ K_m = 0.1,\ Re = 1,\ Gr = 10$ and $N = 0.05$

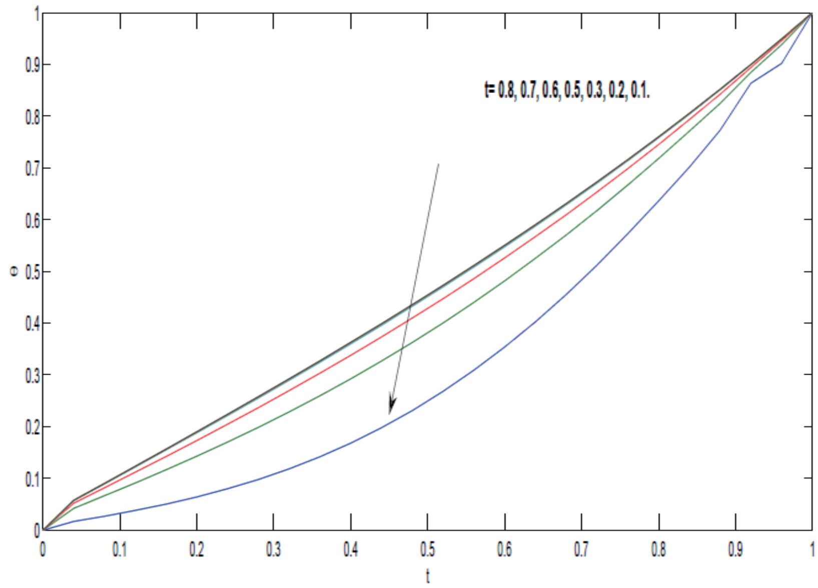

Figure 7. The thermal distribution profiles with variation of time for fixed parameters $Pr = 1.0,\ C = 1,\ M = 20,\ H = 1,\ K_m = 0.1,\ Re = 1,\ Gr = 10$ and $N = 0.05$

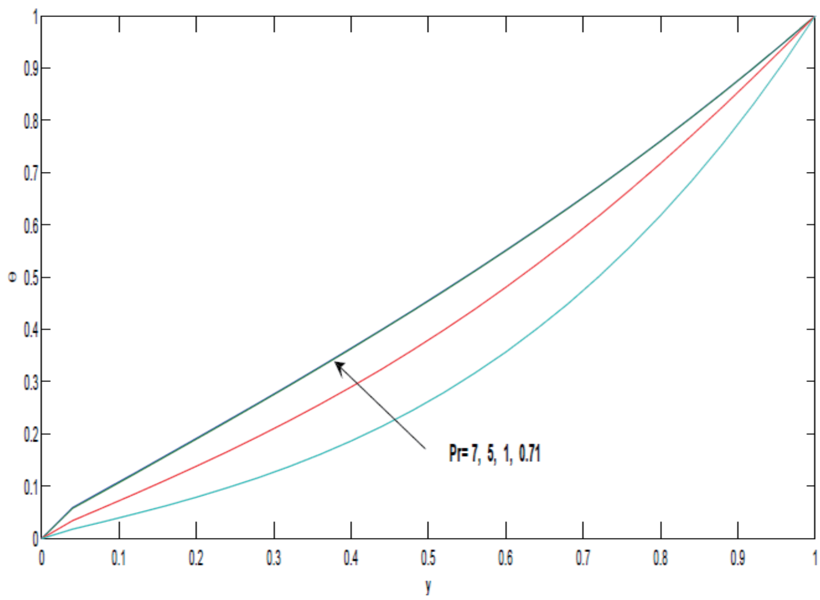

Figure 8. The thermal distribution profiles with variation of praditl number Pr at time $t = 1.0$ and for fixed parameters $C = 1,\ K_m = 0.1,\ M = 20,\ H = 1,\ Re = 1,\ Gr = 10$ and $N = 0.05$

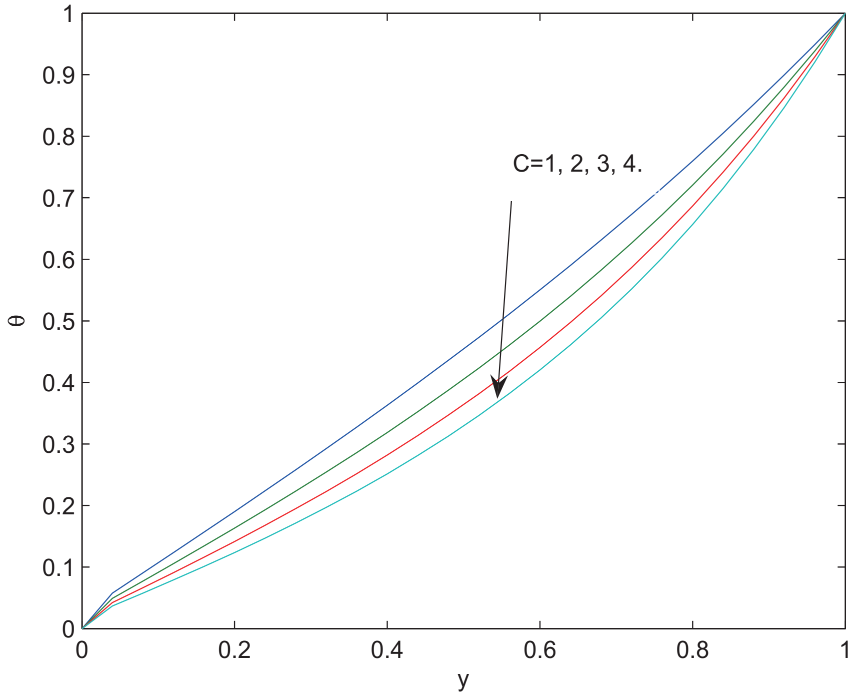

Figure 9. The thermal distribution profiles with variation of radiation parameter C at time $t = 1.0$ and for fixed parameters $Pr = 1.0,\ K_m = 0.1,\ M = 20,\ H = 1,\ Re = 1,\ Gr = 10$ and $N = 0.05$

Table 1. The Skin friction coefficients for various values of K_m, Gr, C, M, Pr, H and N

	$t = 0.5$	$t = 1.0$	$t = 1.5$
$K_m = 0.1$	-0.0079489	-0.0082421	-0.0082495
$K_m = 0.5$	-0.0077783	-0.0080687	-0.00807611
$K_m = 1.0$	-0.0075694	-0.0078563	-0.0078636
$Gr = 2.0$	0.010130	0.010008	0.010004
$Gr = 4.0$	-0.0019226	-0.0021587	-0.002165
$Gr = 8.0$	-0.026028	-0.026493	-0.026503
$C = 2.0$	-0.0045465	-0.004719	-0.0047253
$C = 3.0$	-0.0016936	-0.0017991	-0.0018051
$C = 4.0$	0.00072379	0.00065565	0.00064985
$M = 1.0$	-0.031931	-0.034702	-0.034719
$M = 3.0$	-0.019532	-0.02047	-0.020476
$M = 5.0$	-0.013828	-0.014403	-0.014408
$Pr = 1.0$	-0.0079489	-0.0082421	-0.0082495
$Pr = 5.0$	0.0072287	-0.0022123	-0.0055739
$Pr = 10.0$	0.015887	0.0071173	0.0013746
$H = 2.0$	-0.0067398	-0.007013	-0.0070202
$H = 4.0$	-0.0031324	-0.0033469	-0.0033539
$H = 8.0$	0.0030386	0.002922	0.0029157
$N = 1.0$	-0.0079503	-0.0082436	-0.008251
$N = 10.0$	-0.007964	-0.0082577	-0.0082651
$N = 20.0$	-0.0079793	-0.0082736	-0.008281

Table 2. The Nusselt numbers for various values of C and Pr

	$t = 0.5$	$t = 1.0$	$t = 1.5$
$C = 2.0$	-1.9748	-1.9905	-1.9906
$C = 3.0$	-1.7018	-1.7106	-1.7106
$C = 4.0$	-1.4761	-1.4810	-1.4811
$Pr = 1.0$	-2.3081	-2.3367	-2.3368
$Pr = 5.0$	-0.49401	-1.2048	-1.4751
$Pr = 10.0$	-0.049676	-0.4135	-0.76718

The skin friction coefficient and Nusselt number, as expressed in Equations (8) and (9), are negative of dimensionless velocity and temperature gradients respectively and are shown in Table 1 and Table 2 for various values of fluid parameters. In order to highlight the contributions of each parameter, one parameter is varied while the rest take default fixed values which are $pr = 1.0; cc = 1; Gr = 5; M = 10; H = 1; N = 0.05; K_m = 0.1; re = 1$. It is observed from Table 1 that an increase in any of the parameters Gr and N causes reduction in the skin friction while increasing any of parameters C, M, Pr, K_m and H resulted in coresponding increase in the skin friction coefficient. Practically, the increase in Prandtl number results in an increase in the viscosity of the fluid and thereby decreases the velocity of the fluid. Hence, the dimensionless velocity gradient at the wall decreases with an increase in Prandtl number. Also, increasing buoyancy serves to accelerate the flow which increases the velocity gradient (i.e decrease the skin friction coefficient) in the boundary layer. The rise in radiation parameter reduces velocity gradient at the wall and thereby increasing the coefficient of the skin friction. As for the Nusselt number shown in Table 2, increasing Prandtl number and radiation parameter serve to increase the Nusselt number.It implies that the temperature gradient reduces with a rise in the thermal radiation parameter or Prandtl number Also, The values of the Nusselt number give negative values throughout the time variation as shown in the Table 2. It shows that the temperature inside the fluid is higher than the wall temperature.

5. Conclusion

The effects of radiation and heat transfer on a MHD non-Newtonian unsteady flow in a porous medium with slip condition is presented. The resulting governing equations from the mathematical model of the problem are non-dimensionalised, simplified and solved using Crank Nicolson type of implicit finite difference method. It reveals that temperature increases with a reduction in either the Prandtl number or radiation parameter and that the velocity profile decreases as parameter N, or Grashof number decreases. However, the velocity profile decreases as the value of parameter M, Hartman number or porous parameter increases. Also, it is observed that the velocity and temperature of the fluid increased with the time.

Furthermore, there is a rise in the skin friction due to an increase in Prandtl number, parameter M, magnetic field parameter or radiation parameter while a fall is observed in skin friction with increase in Grashof number or porous parameter K_m.

References

Adesanya, S. O., & Gbadeyan, J. A. (2011). Adomian Decomposition approach to steady Visco-elastic fluid flow with slip through a planar channel. *Journal of Nonlinear Science, 11*(1), 86-94. Retrieved from http://www.internonlinearscience.org/upload/papers/20111011080114712.pdf

Chamkha, A. J. (2007). Heat and mass transfer for non-Newtonian fluid flow along a surface embedded in a porous medium with uniform wall heat and mass fluxes and generation or absorption. *International Journal Of Energy, 3*(1), 97-104. Retrieved from http://www.naun.org/multimedia/NAUN/energy/ijenergy-17.pdf

Chamkha, A. J., Tarkar, H. S., & Soundalgekar, V. M. (2001). Radiation effects on the free convection flow past a semi-infinite vertical plate with mass transfer. *Chemical Engeneering Journal, 84*(3), 335-342. http://dx.doi.org/10.1016/S1385-8947(00)00378-8

Chen, C. H. (2010). On the analytic solution of MHD flow and heat transfer for two types of viscoelastic fluid over a stretching sheet with energy dissipation. *Journal of Heat and Mass Transfer, 53*(19-20), 4264-4273. http://dx.doi.org/10.1016/j.ijheatmasstransfer.2010.05.053

Chen, H. T., & Chen, C. K. (1988). Free convection of non-Newtonian fluids along a vertical plate embedded in a porous medium. *ASME, J. Heat Transfer, 110*, 257-260. http://dx.doi.org/10.1115/1.3250462

Cogley, A. C., Vincentine, W. C., & Gilles, S. E. (1968). Differential approximation for radiative transfer in a non-gray near equilibrium. *AIAA Journal, 6*, 551-555. http://dx.doi.org/10.2514/3.4538

Devika, B., Satya Narayana, P. V., & Venkataramana, S. (2013). MHD oscillatory flow of a Visco Elastic fluid in a porous channel with chemical reaction. *Internation Journal of Engineering Science Invection, 2*(2), 26-35.

Eldabe, N. T. M., Hassan, A., & Mohamed, M. A. A. (2003). Effects of couple stresses on the MHD of a non-Newtonian unsteady fiow between two parallel porous plates. *Verlag der Zeitschrift fur Naturforschung, Tubingen, 58*(a), 204-210. Retrieved from http://www.znaturforsch.com/aa/v58a/s58a0204.pdf

Grosan, T., & Pop, I. (2001). Free convection over a vertical flat with a variable wall temperature and Internal Heat Generation in a porous medium saturated with a non-Newtonian fluid. *Technische Mechanik, 21*(4), 313-318.

Hsieh, J. C., Chen, T. S., & Armarly, B. F. (1993). Non-Similarity solutions for mixed convection from vertical surface in a porous medium. *Int. J. Heat Mass Transfer, 36*, 1485-1493. http://dx.doi.org/10.1016/S0017-9310(05)80059-6

Mehta, K. N., & Rao, K. N. (1994). Buoyancy-induced flow of non-Newtonian fluids in porous medium past a vertical plate with non-uniform surface heat flux. *Int. J. Eng. Sci., 32*(3), 521-525. http://dx.doi.org/10.1016/0020-7225(94)90138-4

Mehta, K. N., & Rao, K. N. (1994). Buoyancy induced flow of non-Newtonian fluids over a non-isothermal horizontal plate embedded in a porous medium. *Int. J. Eng. Sci., 27*, 1025-1035.

Mohanmmadein, A. A., & El-Amin, M. F. (2000). Thermal radiation effects on power-law fluid over a horizontal plate embedded in a porous medium. *Int. Comm. Heat Transfer, 27*(7), 1025-1035. http://dx.doi.org/10.1016/S0735-1933(00)00182-2

Okoya, S. S. (2008). On the transition for a generalised couette flow of a reactive third-grade fluid with viscous dissipation. *International Communication in heat and Mass Transfer, 35*, 188-196. http://dx.doi.org/10.1016/j.icheatmasstransfer.2007.06.012

Okoya, S. S. (2011). Disappearance of criticality for a reactive third-grade fluid with Reynolds model viscosity in a flat channel. *International Journal of Non-linear Mechanics, 46*, 1110-1115. http://dx.doi.org/10.1016/j.ijnonlinmec.2011.04.008

Ranganathan, P., & Viskanta, R. (1984). Mixed convection boundary layer flow along a vertical surface in a porous medium. *Numerical Heat Transfer, 7*, 305-317.

Shobha, & Chandrashekar, N. (2012). Free convection in a non-Newtonian fluid along a horizontal plate embedded in a porous medium with internal heat generation. *International Communication in Heat and Mass transfer, 39*, 537-540. http://dx.doi.org/10.1016/j.icheatmasstransfer.2012.02.003